



OPEN 1H-MRS parameters in non-enhancing peritumoral regions can predict the recurrence of glioblastoma

Wenchao Lu^{1,2,3}, Jin Feng^{2,3}, Yourui Zou², Yang Liu², Peng Gao², Yang Zhao¹, Xiao Wu¹ & Hui Ma²✉

This study aimed to evaluate the predictive value of metabolic parameters in preoperative non-enhancing peritumoral regions (NEPTRs) for glioblastoma recurrence, using multivoxel hydrogen proton magnetic resonance spectroscopy (1H-MRS). Clinical and imaging data from patients with recurrent glioblastoma were analyzed. Through co-registration of preoperative and post-recurrence MRI, we identified future tumor recurrence regions (FTRRs) and future non-tumor recurrence regions (FNTRRs) within the NEPTRs. Metabolic parameters were recorded separately for each region. Cox regression analysis was applied to assess the association between metabolic parameters and glioblastoma recurrence. Compared to FNTRRs, FTRRs exhibited a higher Cho/Cr ratio, higher Cho/NAA ratio, and lower NAA/Cr ratio. Both Cho/NAA and Cho/Cr ratios were recognized as risk factors in univariate and multivariate analyses ($P < 0.05$). The Cox regression model indicated that Cho/NAA > 1.99 and Cho/Cr > 1.73 are independent risk factors for early glioblastoma recurrence. Based on these cut-off values, patients were stratified into low-risk and high-risk groups, with a statistically significant difference in recurrence rates between the two groups ($P < 0.01$). The Cho/NAA and Cho/Cr ratios in NEPTRs are independent predictors of future glioblastoma recurrence. Specifically, Cho/NAA > 1.99 and/or Cho/Cr > 1.73 in NEPTRs may indicate a higher risk of early postoperative recurrence at these regions.

Keywords Glioblastoma, Magnetic resonance spectroscopy, Choline, Non-enhancing peritumoral regions, Recurrence

Glioblastoma is the most common primary malignant brain tumor in adults¹. Standard treatment for newly diagnosed glioblastoma includes surgical resection, followed by adjuvant radiotherapy and chemotherapy². Maximizing safe tumor resection remains the cornerstone of glioblastoma surgery and is crucial for improving patient prognosis^{3,4}. Clinically, the extent of resection is typically assessed using MRI T1-enhanced imaging. Despite achieving complete resection in most cases, as indicated by T1-enhanced images, recurrence rates remain high, and survival outcomes are often suboptimal^{5,6}. Notably, glioblastoma recurrence frequently occurs in the non-enhancing peritumoral regions (NEPTRs)⁷, which consist of complex cellular and molecular components⁸. In recent years, NEPTRs have garnered increasing attention from clinicians; however, focused research on these regions remains limited.

Multivoxel hydrogen proton magnetic resonance spectroscopy (1H-MRS) is widely used to noninvasively assess biochemical markers and metabolic changes within intracranial lesions. This technique plays a vital role in the differential diagnosis and prognostic evaluation of glioma patients⁹. The imaging characteristics provided by multivoxel 1H-MRS can reveal the heterogeneity in tumor cell distribution and metabolic activity within the NEPTRs of glioblastoma at a voxel-specific level¹⁰. Early identification of NEPTRs at elevated risk for future recurrence on preoperative MRS imaging is essential for facilitating timely intervention and potentially reducing tumor recurrence.

¹First School of Clinical Medicine, Ningxia Medical University, Yinchuan 750004, Ningxia Hui Autonomous Region, China. ²Department of Neurosurgery, General Hospital of Ningxia Medical University, No. 804 Shengli South Street, Yinchuan 750004, Ningxia Hui Autonomous Region, China. ³The authors contribute equally. ✉email: Mahui0528@aliyun.com

Currently, relatively few studies have examined the association between MRS findings and glioblastoma recurrence within the heterogeneous NEPTRs of preoperative glioblastoma^{11,12}. Further research is needed to clarify the potential of preoperative MRS in identifying high-risk subregions within NEPTRs that are prone to future recurrence. This study aims to compare the metabolic parameters between regions of future tumor recurrence and non-recurrence within the non-enhancing peritumoral area on preoperative imaging and to explore the clinical significance of these parameters in predicting tumor recurrence.

Materials and methods

Patients

We retrospectively analyzed clinical and imaging data from 195 patients diagnosed with glioblastoma who were admitted to our hospital between August 2019 and December 2023. All patient-identifying information was anonymized. Based on inclusion and exclusion criteria, 52 patients were ultimately included in the study, comprising 35 males (67.3%) and 17 females (32.7%), with a mean age of 53.8 ± 10.9 years. All tumors were located supratentorially. The average tumor size was 4.9 ± 1.3 cm, with gross-total resection (GTR) achieved in 46 patients (88.5%) and near-total resection (NTR) in 6 patients (11.5%). Chromosome 1p/19q codeletion was observed in 2 patients (3.8%), and O6-methylguanine-DNA-methyltransferase (MGMT) promoter methylation was detected in 25 patients (48%).

Ethics approval and consent to participate

This study was approved by the Medical Ethics Committee of the General Hospital of Ningxia Medical University (approval no. KYLL-20240309) and complied with the ethical standards outlined in the Declaration of Helsinki for medical research involving human subjects. The requirement for informed consent was waived by the committee due to the retrospective design of the study.

Inclusion criteria

(a) Patients diagnosed with glioma who underwent surgical treatment. (b) Patients with complete imaging data, including preoperative conventional MRI, multivoxel ¹H-MRS, and postoperative MRI performed within 72 h. (c) Patients diagnosed with glioblastoma according to the World Health Organization (WHO) classification for central nervous system tumors. (d) Patients who received radiotherapy and temozolomide treatment following tumor resection. (e) Patients with confirmed evidence of tumor recurrence on follow-up MRI scans.

Exclusion criteria

(a) Patients with indeterminate enhancing lesions, such as pseudoprogression or post-radiation necrosis. (b) Patients with glioblastoma recurrence occurring outside the initial surgical site. (c) Patients lacking sufficient sequential MRI follow-up at our institution prior to glioblastoma recurrence. (d) Patients with incomplete clinical information.

Criteria for glioblastoma recurrence

Glioblastoma recurrence was assessed using postoperative follow-up MRI, applying the diagnostic criteria established by the Response Assessment in Neuro-Oncology (RANO) Working Group¹³, or confirmed through histopathological findings from reoperation. MRI evaluations were conducted by two independent neuroradiologists blinded to study outcomes.

Imaging data

MRI data acquisition was performed for all patients using a GE Signa 3.0 T Magnetic Resonance Imaging (MRI) system equipped with a 16-channel cranial-specific coil. Patients were positioned supine, and routine MRI scans in axial, coronal, and sagittal planes were obtained. These scans included T1-weighted, T2-weighted, multivoxel ¹H-MRS, T2-FLAIR, and T1 contrast-enhanced sequences.

Multivoxel ¹H-MRS data were acquired using a three-dimensional point-resolved spectroscopy (PRESS) sequence with the following acquisition parameters: echo time (TE): 144 ms, repetition time (TR): 2000 ms, field of view (FOV): 160 mm × 160 mm, slice thickness of 10 mm, voxel size: 10 mm × 10 mm × 10 mm, number of excitations (NEX): 1, and an average of 3, with a scan time of 6 min and 53 s. The spectral bandwidth was set at 2000 Hz, with 1024 data points. Automatic shimming and water suppression were applied before MRS acquisition, and MRS scanning was performed prior to gadolinium injection to minimize any influence of gadolinium agents on metabolic parameters.

MRS image processing

Raw MRS data were processed using FuncTool software, which performed phase correction, signal filling, and data analysis. Both baseline and phase corrections were automatically conducted by the software. Based on the preselected region of interest, the workstation generated multi-voxel MRS spectral lines.

Region of interest (ROI) selection

The regions of interest (ROIs) in this study were defined as the future tumor recurrence regions (FTRRs) and future non-tumor recurrence regions (FNTRRs) within the NEPTRs. These ROIs were created by co-registering the contrast-enhanced T1 MRI at the time of tumor recurrence with the preoperative contrast-enhanced T1 MRI. The entire process was completed using a two-stage semi-automated nonlinear registration method based on FMRIB Software Library (FSL) version 6.0.7 (<http://fsl.fmrib.ox.ac.uk/fsl/fslwiki/>)¹⁴, following previously described methods¹⁵. The specific steps were as follows: First, we applied linear FLIRT co-registration to calculate the transformation matrix between the preoperative tumor mass and the postoperative resection cavity. Next,

we applied this transformation matrix using nonlinear FNIRT transformation to align the brain structures. By subtracting the preoperative contrast-enhanced lesion, we identified the FTRRs and FNTRRs on the preoperative MRI¹⁶. Subsequently, the metabolite ratios for these regions were extracted from the preoperative MRS data. Additionally, we mirrored the FTRRs to obtain a control area representing normal brain tissue and recorded its metabolite ratios (Fig. 1).

Observation indicators

The association between multivoxel ¹H-MRS metabolic parameters (Cho/Cr, Cho/NAA, NAA/Cr) in the preoperative ROIs and glioblastoma recurrence was evaluated. Additionally, the predictive efficacy of these metabolic parameters for postoperative glioblastoma recurrence was assessed using receiver operating characteristic (ROC) curve analysis.

Statistical analysis

Statistical analyses were performed using IBM SPSS Statistics 23.0 (IBM Corporation, Armonk, NY, USA) and R software (version 4.3.2), with the R packages “multipleROC,” “survival,” and “survminer.” Continuous data were expressed as mean ± standard deviation (SD), and categorical variables were presented as percentages. Paired t-tests were used for comparisons between subgroups. Univariate and multivariate Cox regression analyses were conducted to identify risk factors associated with glioblastoma recurrence. Receiver operating characteristic (ROC) curves were constructed to determine the area under the curve (AUC) and optimal cut-off values for metabolic ratios in predicting glioblastoma recurrence. The Kaplan–Meier method was used to plot non-recurrence rate curves over time, and log-rank tests were applied to compare Kaplan–Meier curves. A P-value < 0.05 was considered statistically significant for all analyses (Table 1).

Results

Comparison of metabolic parameters in different ROIs

Multivoxel ¹H-MRS metabolic parameters were analyzed and compared among the FTRRs, FNTRRs within NEPTRs, and the normal control regions (NCRs) (Fig. 2). The Cho/Cr and Cho/NAA ratios in NEPTRs with FTRRs were significantly higher than those in NEPTRs with FNTRRs (1.83 ± 0.25 vs. 1.34 ± 0.25 , $p < 0.001$; 2.09 ± 0.24 vs. 1.07 ± 0.23 , $p < 0.001$) and NCRs (1.83 ± 0.25 vs. 1.20 ± 0.15 , $p < 0.001$; 2.09 ± 0.24 vs. 0.92 ± 0.17 , $p < 0.001$). The NAA/Cr ratio in NEPTRs with FTRRs was significantly lower than that in NEPTRs with FNTRRs (1.10 ± 0.21 vs. 2.27 ± 0.18 , $p < 0.001$) and NCRs (1.10 ± 0.21 vs. 2.38 ± 0.31 , $p < 0.001$). Additionally, the Cho/Cr and Cho/NAA ratios in NEPTRs with FNTRRs were significantly higher than those in NCRs (1.34 ± 0.25 vs.

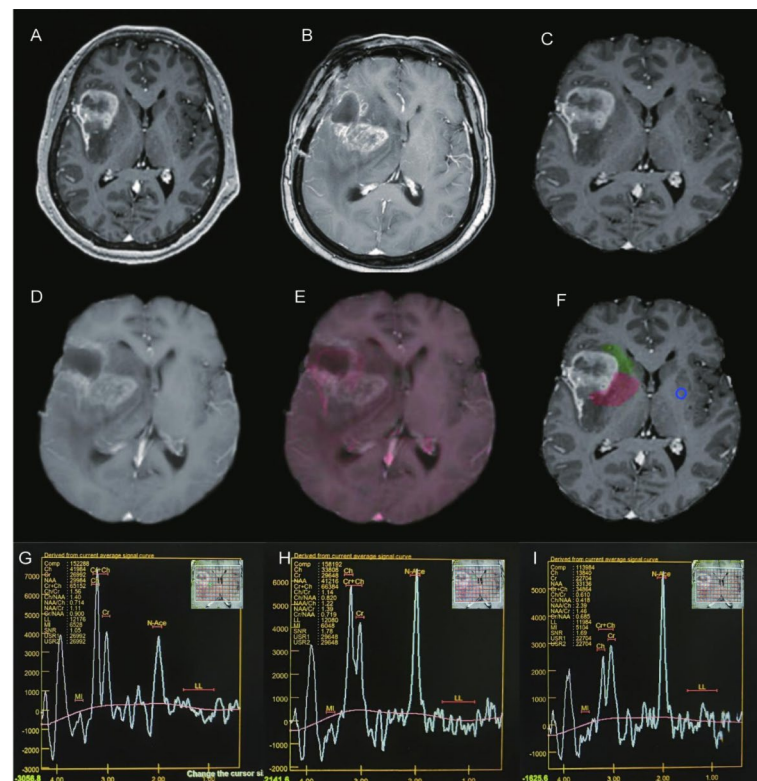


Fig. 1. Use co-registration technology to register preoperative (A) and postoperative (B) MRI images. By registering the images (C, D, E), it is possible to further clarify the future tumor recurrence (F, red) and non tumor recurrence regions (F, green) in the NEPTRs, and thus obtain ¹H-MRS parameters for different regions (G: future tumor recurrence; H: non tumor recurrence regions, I: normal control regions, blue).

Demographics	No. of patients (%)
Gender	
Male	35 (67.3)
Female	17 (32.7)
Age (years)	
Mean \pm SD	53.8 \pm 10.9
Tumor size (cm)	
Mean \pm SD	4.9 \pm 1.3
Extent of resection	
GTR	46 (88.5)
NTR	6 (11.5)
1p/19q codeletion	
Yes	2 (3.8)
No	50 (96.2)
MGMT methylation	
Yes	25 (48.1)
No	27 (51.9)

Table 1. Baseline characteristics for all patients with Recurrent glioblastoma. GTR: gross-total resection; NTR: near-total resection; SD: standard deviation; MGMT: O6-methylguanine-DNA-methyltransferase.

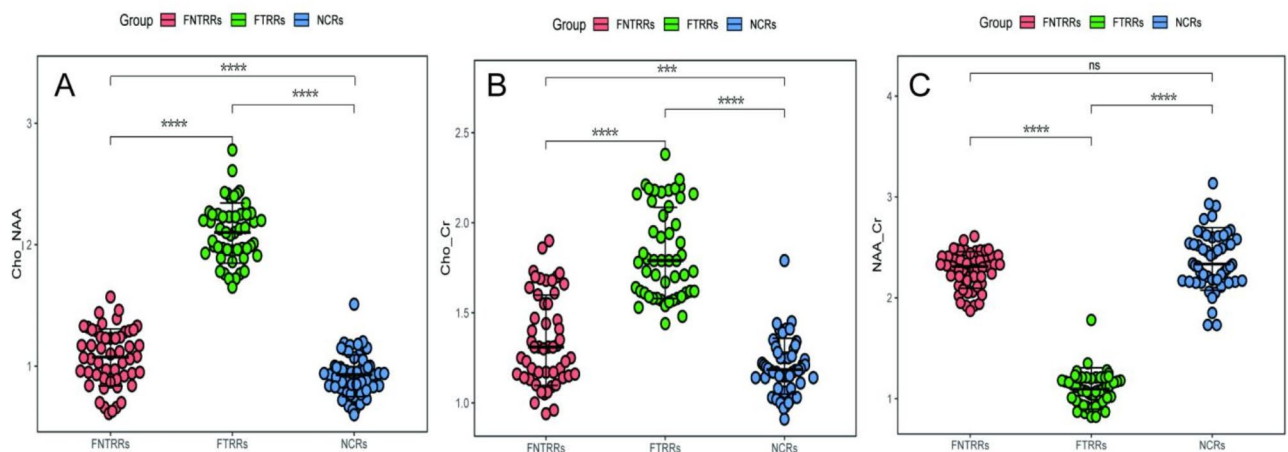


Fig. 2. Comparison of 1H-MRS metabolic parameters in FNTRRs, FTRRs and NCRs. The Cho/Cr and Cho/NAA ratios in the FTRRs are significantly increased, while the NAA/Cr ratios are significantly decreased. Compared with the FNTRRs and the NCRs. The Cho/Cr and Cho/NAA ratios in the FNTRRs were significantly higher than those in the NCRs. Although the NAA/Cr ratios in the FNTRRs were lower than those in the NCRs, there was no statistical significance between the two regions ($p = 0.053$). **** $p < 0.0001$, *** $p < 0.001$, ^{ns} $p > 0.05$. *MRS: magnetic resonance spectroscopy; FTRRs: future tumor recurrence regions; FNTRRs: future non-tumor recurrent regions; NCRs: normal control regions.

1.20 ± 0.15 , $p < 0.001$; 1.07 ± 0.23 vs. 0.92 ± 0.17 , $p < 0.001$). Although the NAA/Cr ratio was lower in NEPTRs with FNTRRs compared to NCRs, this difference was not statistically significant (2.27 ± 0.18 vs. 2.38 ± 0.31 , $p = 0.053$).

Univariate and multivariate cox regression analysis

Univariate analysis revealed that age, extent of tumor resection, and the Cho/Cr and Cho/NAA ratios were significantly associated with glioblastoma recurrence ($P < 0.05$) (Table 2). These factors were subsequently included in the multivariate Cox regression analysis. In the Cox proportional hazards model, extent of resection (HR = 0.112, 95% CI: 0.036–0.344, $P < 0.001$), Cho/Cr ratio (HR = 4.977, 95% CI: 1.236–20.027, $P = 0.023$), and Cho/NAA ratio (HR = 20.832, 95% CI: 4.937–87.907, $P < 0.001$) were identified as independent predictors of glioblastoma recurrence. Based on the final multivariate model, a nomogram was developed by assigning weighted scores to each recurrence-associated factor. This nomogram was used to determine the total score and probability of glioblastoma recurrence for patients in the cohort (Fig. 3).

Variable	Univariate analysis			Multivariate analysis		
	HR	95% CI	P-value	HR	95% CI	P-value
Gender	0.542	0.297–0.988	0.046	1.301	1.015–1.114	0.154
Age	1.028	1.001–1.057	0.043	1.034	1.005–1.064	0.179
Tumor Size	0.970	0.754–1.248	0.832			
Extent of resection	0.130	0.049–0.347	<0.001	0.112	0.036–0.344	<0.001
1p/19q codeletion(yes/no)	0.771	0.186–3.196	0.72			
MGMT methylation (yes/no)	0.974	0.549–1.730	0.929			
Cho/Cr	6.702	2.094–21.451	0.001	4.977	1.236–20.027	0.023
Cho/NAA	24.752	6.419–95.432	<0.001	20.832	4.937–87.907	<0.001
NAA/Cr	0.397	0.067–2.377	0.311			

Table 2. Univariate and multivariate analysis in all patients. HR, hazard ratio; CI, confidence interval; MGMT, O6-methylguanine-DNA-methyltransferase; NAA, N-acetyl-aspartate; Cho, choline; Cr, creatine.

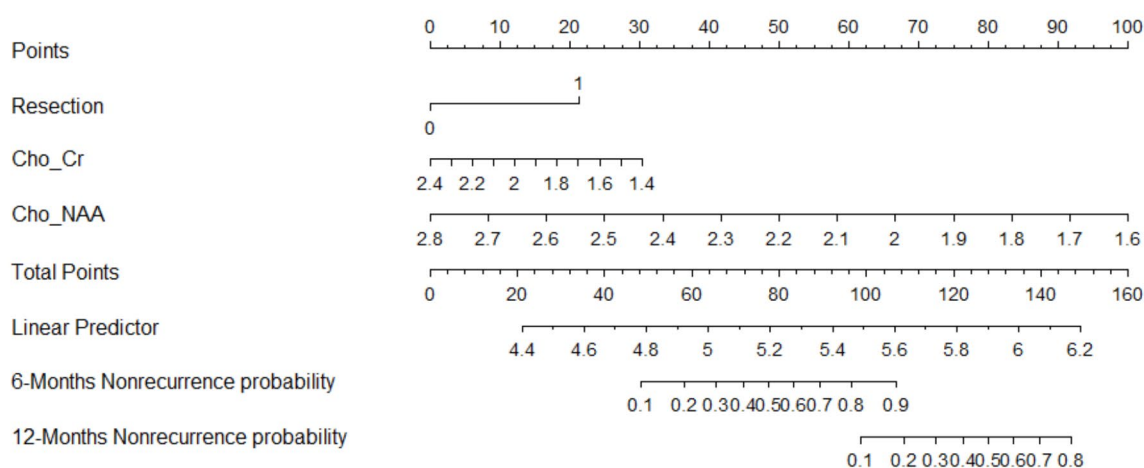


Fig. 3. Characteristics in the nomogram to predict probability of tumor recurrence in patients with glioblastoma. *Reaction: 1: gross-total resection; 0: near-total resection, NAA, N-acetyl-aspartate; Cho, choline; Cr, creatine.

Value of MRS metabolic parameters in predicting glioblastoma recurrence

The Cho/Cr and Cho/NAA ratios were identified as independent risk factors for glioblastoma recurrence. To further explore the predictive value of ¹H-MRS metabolic parameters, we conducted ROC curve analysis to establish optimal cutoff values for Cho/NAA, Cho/Cr, and NAA/Cr ratios, and assessed their predictive performance. The median time to glioblastoma recurrence in our cohort was 260 days, which was used as the segmentation point. Based on ROC analysis, a cutoff value of 1.99 for the Cho/NAA ratio was identified, yielding an AUC of 0.848 (95% CI: 0.732–0.963, $P < 0.001$). For the Cho/Cr ratio, the critical threshold was 1.73, with an AUC of 0.704 (95% CI: 0.552–0.856, $P < 0.001$). For the NAA/Cr ratio, the cutoff was 1.17, with an AUC of 0.663 (95% CI: 0.505–0.829, $P < 0.001$) (Fig. 4).

Glioblastoma recurrence prediction model

The Cho/NAA and Cho/Cr ratios demonstrated strong predictive value for glioblastoma recurrence, with optimal cutoff values established. Based on these cutoff values, patients were stratified into high-risk and low-risk groups. A comparison of future non-recurrence rates between the two groups revealed a statistically significant difference ($P = 0.009$ for Cho/NAA; $P = 0.002$ for Cho/Cr), as anticipated (Fig. 5).

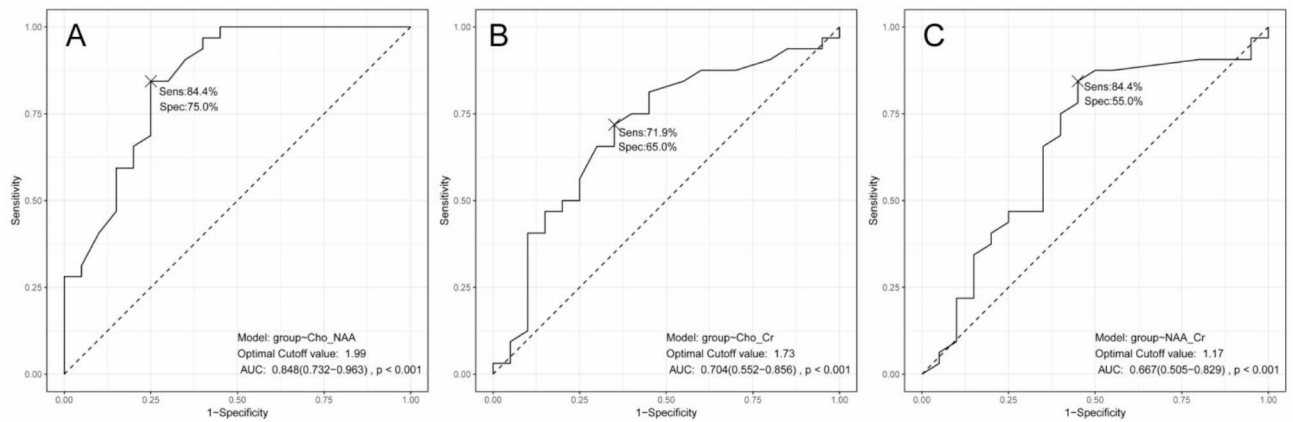


Fig. 4. ROC curves displaying the metabolic ratios: Cho/NAA (A), Cho/Cr (B), and NAA/Cr (C) in recurrence prediction. The cutoff ratio of Cho/NAA was 1.99 with an area under the curve (AUC) of 0.848 ($P < 0.001$). The cutoff ratio of Cho/Cr was 1.73 with an AUC of 0.704 ($P < 0.001$). The cutoff ratio of NAA/Cr was 1.17 with an AUC of 0.667 ($P < 0.001$).

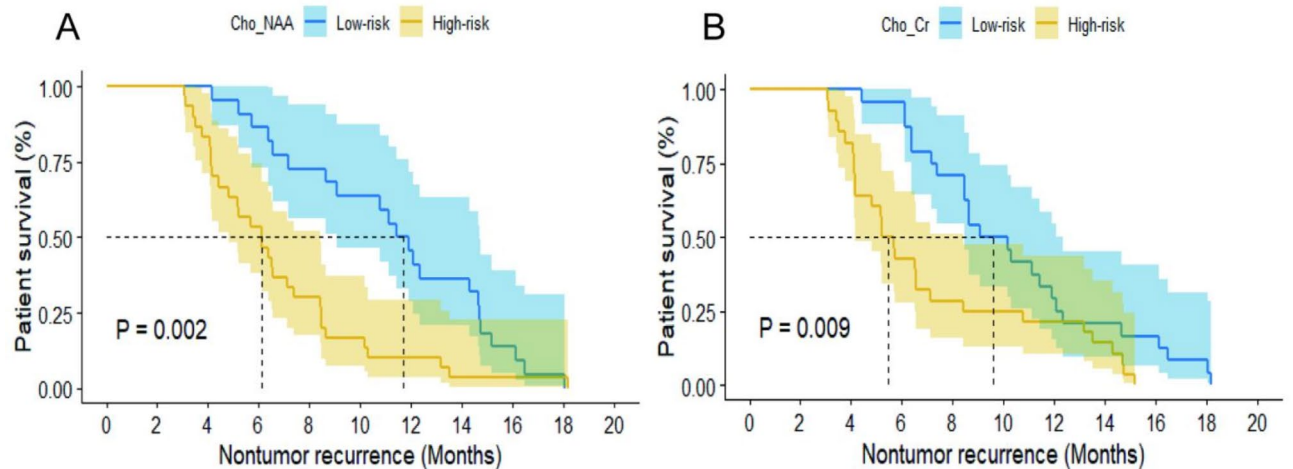


Fig. 5. Comparison of recurrence probabilities between different subgroups based on the optimal cutoff. (A) There was a statistical difference in the recurrence probabilities between patients in low-Cho/Cr and high-Cho/Cr groups ($P = 0.009$). (B) The difference in recurrence probability between low Cho/NAA and high Cho/NAA groups is statistically significant ($P = 0.002$).

Discussion

Glioblastoma is widely recognized as the most aggressive and prevalent primary brain tumor¹. Despite advancements in surgical and therapeutic approaches, glioblastoma recurrence remains almost inevitable¹⁷, with up to 90% of recurrences occurring at or near the surgical resection site¹⁵. This poor prognosis largely results from local treatment failure, often due to the dependence on contrast-enhanced T1-weighted imaging to assess the extent of resection in glioblastoma patients. Currently, complete resection of the contrast-enhanced tumor region is typically viewed as an indicator of gross total resection^{18–20}. Studies have shown a significant correlation between glioblastoma recurrence and infiltrating tumor cells within NEPTRs. These regions provide a niche where glioblastoma cells can infiltrate and intermingle with peritumoral edema^{21–24}. Additionally, both the extent and degree of edema within NEPTRs are associated with the malignancy level and may serve as predictors of patient prognosis^{25,26}. Thus, understanding methods for monitoring changes in tumor burden within NEPTRs is critical.

The multivoxel ¹H-MRS technique is a noninvasive imaging method with significant potential for assessing tumor tissue metabolism²⁷. In this study, we systematically analyzed MRS parameters within NEPTRs and found that glioblastoma NEPTRs with future tumor recurrence displayed elevated Cho/Cr and Cho/NAA ratios, along with reduced NAA/Cr ratios. Multivariate analysis confirmed that Cho/Cr and Cho/NAA ratios are independent risk factors for future tumor recurrence within NEPTRs. Choline serves as an indicator of cell proliferation and membrane turnover, with elevated choline levels reflecting heightened tumor cell activity. Conversely, reduced

NAA levels correspond to severe neuronal damage²⁸. Thus, elevated Cho/Cr and Cho/NAA values suggest increased tumor cell activity and significant neuronal destruction within these regions²⁹.

Tomasz Czernicki et al.³⁰ reported that changes in MRS metabolite ratios can help confirm glioma recurrence. Specifically, the presence of substantial contrast enhancement on postoperative MRI, along with an increased Cho/NAA ratio and decreased NAA/Cr ratio on MRS, raises initial suspicion of glioma recurrence. Similarly, Stephen et al.³¹ demonstrated that combining MRS with DTI allows for the detection of changes in both invasive and non-invasive tumor regions, with significantly higher Cho/Cr and Cho/NAA levels and lower NAA/Cr levels observed in invasive areas surrounding the tumor compared to non-invasive areas. These findings are consistent with our study's observations regarding MRS parameter changes. Elevated Cho/Cr and Cho/NAA ratios in NEPTRs with FTRRs suggest a higher density and metabolic activity of glioblastoma cells within these regions. Therefore, our findings, alongside previous studies^{30,32–34}, suggest that elevated Cho/Cr and Cho/NAA ratios in NEPTRs may serve as potential indicators of future glioblastoma recurrence.

Additionally, Cepeda et al.³⁵ developed a predictive model for glioblastoma recurrence by extracting preoperative and follow-up MRI data using the Cancer Imaging Phenomics Toolkit (CaPTk). This model incorporated T1-weighted (T1w), T2-weighted (T2w), FLAIR, T1w contrast-enhanced (T1ce) sequences, and diffusion-weighted imaging-derived apparent diffusion coefficient (ADC) values. While the model assesses recurrence prediction, it does not address the relationship between MRS metabolic parameters and tumor recurrence. Yan et al.¹⁵ used FSL software to compare preoperative and recurrent MRI images in glioblastoma patients, identifying unique features in preoperative MRI that indicate potential areas of progression. They found higher Cho/NAA and lower NAA ratios in regions of peritumoral progression compared to non-progressing regions, although these differences did not reach statistical significance. Cui et al.³⁶ demonstrated a significant increase in the Cho/Cr and Cho/NAA ratios and a marked decrease in the NAA/Cr ratio when comparing recurrent MRI with postoperative MRS. They concluded that an elevated Cho/NAA ratio within the peritumoral edema region of glioblastoma predicted early recurrence and was associated with a poor prognosis. However, it is important to note that their predictions regarding tumor recurrence were based on MRS parameters obtained within 72 h post-surgery, which introduces limitations. Surgical trauma in the operative area can significantly influence MRS parameters and may not accurately reflect the true metabolic state of NEPTRs.

Moreover, variations in results may arise due to individual tumor characteristics and different interpretations of surgical resection extent among surgeons. However, as all surgeries in our study were performed by the same surgical team at our center, we minimized variability due to differing surgical interpretations. Additionally, to enhance the study of glioblastoma recurrence in relation to MRS metabolic parameters, we achieved precise co-registration of postoperative and preoperative MRI using a two-stage nonlinear semi-automated co-registration method. This enabled us to identify prospective FTRRs and FNTRRs within NEPTRs on preoperative MRI and extract their metabolic parameters from preoperative MRS data, resulting in findings that more accurately reflect patient data. Furthermore, we developed a nomogram that incorporates risk factors for future recurrence within NEPTRs, providing a tool for early prediction of glioblastoma recurrence. This predictive model may assist clinicians in optimizing treatment plans and identifying high-risk areas for surgical intervention.

To further clarify the predictive value of Cho/Cr (optimal cutoff = 1.73) and Cho/NAA (optimal cutoff = 1.99) for glioblastoma recurrence, we stratified patients into low-risk and high-risk subgroups based on these cutoffs. Analysis of these two cohorts revealed a significantly higher tumor recurrence rate in the high-risk group compared to the low-risk group. In their study on glioblastoma recurrence and radiation necrosis, Feng et al.³⁷ reported a significant elevation in Cho/NAA levels associated with tumor recurrence, with an AUC of 0.940; however, they did not specify cutoff values for Cho/NAA in predicting recurrence. Cui et al.³⁶ found that the Cho/NAA and NAA/Cr ratios were optimal predictors for glioblastoma recurrence, with AUC values of 0.731 and 0.754, respectively, although the Cho/Cr ratio demonstrated limited predictive capability (AUC = 0.541). Their analysis suggested that a Cho/NAA ratio ≥ 1.31 indicated early tumor recurrence; however, these findings were based on postoperative MRS parameters and had relatively low AUC values, limiting their relevance as preoperative clinical references. In contrast, our proposed model, based on preoperative MRS parameters, offers greater stability and practical value in preoperative clinical settings, providing a more reliable tool for predicting glioblastoma recurrence.

Limitations

This study has several limitations: First, the analysis was constrained by the small sample size, highlighting the need for larger, prospective studies to further assess the impact of different parameters on glioblastoma recurrence. Second, in most cases, tumor recurrence diagnosis relied solely on follow-up MRI images without sufficient histopathological confirmation. Third, postoperative resorption of the surgical cavity, along with peripheral scarring and gliosis formation, may introduce timing discrepancies between recurrent and preoperative MRI image alignment. To minimize the impact of this bias, a two-stage co-registration method was employed in this study. Despite these limitations, our study presents notable findings that may inform the development of treatment protocols using preoperative MRS to facilitate early detection of recurrence in glioblastoma patients.

Conclusion

The Cho/NAA and Cho/Cr ratios within the NEPTRs of glioblastoma are effective predictors of future tumor recurrence. A Cho/NAA ratio exceeding 1.99 and/or a Cho/Cr ratio surpassing 1.73 in NEPTRs indicates a higher likelihood of recurrence in these regions. Utilizing preoperative NEPTR metabolic parameters in glioblastoma allows for a more accurate prediction of recurrence, enabling timely adjustments to treatment plans to improve patient outcomes.

Data availability

The data sets used and/or analyzed in this study are available from the corresponding author on reasonable request.

Received: 24 June 2024; Accepted: 19 November 2024

Published online: 26 November 2024

References

- Ostrom, Q. T. et al. CBTRUS statistical report: Primary brain and other central nervous system tumors diagnosed in the United States in 2015–2019. *Neuro Oncol.* **24**(Suppl 5), v1–v95. <https://doi.org/10.1093/neuonc/noac202> (2022).
- McMahon, D. J. et al. Management of newly diagnosed glioblastoma multiforme: current state of the art and emerging therapeutic approaches. *Med Oncol.* **39**(9), 129. <https://doi.org/10.1007/s12032-022-01708-w> (2022).
- Czarnywojtek, A. et al. Glioblastoma multiforme: The latest diagnostics and treatment techniques. *Pharmacology.* **108**(5), 423–431. <https://doi.org/10.1159/000531319> (2023).
- Yan, J. et al. Extent of resection of peritumoral diffusion tensor imaging-detected abnormality as a predictor of survival in adult glioblastoma patients. *J Neurosurg.* **126**(1), 234–241. <https://doi.org/10.3171/2016.1.JNS152153> (2017).
- Jiang, H. et al. Proliferation-dominant high-grade astrocytoma: survival benefit associated with extensive resection of FLAIR abnormality region. *J Neurosurg.* **132**(4), 998–1005. <https://doi.org/10.3171/2018.12.JNS182775> (2019).
- Brown, T. J. et al. Association of the extent of resection with survival in glioblastoma: A systematic review and meta-analysis. *JAMA Oncol.* **2**(11), 1460–1469. <https://doi.org/10.1001/jamaoncol.2016.1373> (2016).
- Ziwei, Tu. et al. Limited recurrence distance of glioblastoma under modern radiotherapy era. *BMC Cancer.* **21**(1), 720. <https://doi.org/10.1186/s12885-021-08467-3> (2021).
- Ballestin, A. et al. Peritumoral brain zone in glioblastoma: Biological, clinical and mechanical features. *Front Immunol.* **15**, 1347877. <https://doi.org/10.3389/fimmu.2024.1347877> (2024).
- Kumar, M. et al. Emerging MR imaging and spectroscopic methods to study brain tumor metabolism. *Front Neurol.* **16**(13), 789355. <https://doi.org/10.3389/fneur.2022.789355> (2022).
- Martín-Noguerol, T. et al. Advanced MRI assessment of non-enhancing peritumoral signal abnormality in brain lesions. *Eur J Radiol.* **143**, 109900. <https://doi.org/10.1016/j.ejrad.2021.109900> (2021).
- Talati, P. et al. MR spectroscopic imaging predicts early response to anti-angiogenic therapy in recurrent glioblastoma. *Neurooncol Adv.* **3**(1), vdab060. <https://doi.org/10.1093/noonl/vdab060> (2021).
- Bulik, M. et al. The diagnostic ability of follow-up imaging biomarkers after treatment of glioblastoma in the temozolomide era: Implications from proton MR spectroscopy and apparent diffusion coefficient mapping. *Biomed Res Int.* **2015**, 641023. <https://doi.org/10.1155/2015/641023> (2015).
- Nayak, L. et al. The Neurologic Assessment in Neuro-Oncology (NANO) scale: A tool to assess neurologic function for integration into the Response Assessment in Neuro-Oncology (RANO) criteria. *Neuro Oncol.* **19**(5), 625–635. <https://doi.org/10.1093/neuonc/nox029> (2017).
- Jenkinson, M. et al. FSL. *Neuroimage* **62**(2), 782–790. <https://doi.org/10.1016/j.neuroimage.2011.09.015> (2012).
- Yan, J. et al. A neural network approach to identify the peritumoral invasive Areas in Glioblastoma patients by Using MR Radiomics. *Sci Rep.* **10**(1), 9748. <https://doi.org/10.1038/s41598-020-66691-6> (2020).
- van der Hoorn, A. et al. Validation of a semi-automatic co-registration of MRI scans in patients with brain tumors during treatment follow-up. *NMR Biomed.* **29**(7), 882–889. <https://doi.org/10.1002/nbm.3538> (2016).
- Mallick, S., Benson, R., Hakim, A. & Rath, G. K. Management of glioblastoma after recurrence: A changing paradigm. *J Egypt Natl Cancer Inst.* **28**(4), 199–210. <https://doi.org/10.1016/j.jnci.2016.07.001> (2016).
- Osorio, J. A. & Aghi, M. K. Optimizing glioblastoma resection: intraoperative mapping and beyond. *CNS Oncol.* **3**(5), 359–366. <https://doi.org/10.2217/cns.14.36> (2014).
- Oppenlander, M. E. et al. An extent of resection threshold for recurrent glioblastoma and its risk for neurological morbidity. *J Neurosurg.* **120**(4), 846–853. <https://doi.org/10.3171/2013.12> (2014).
- Ellingson, B. M., Wen, P. Y. & Cloughesy, T. F. Evidence and context of use for contrast enhancement as a surrogate of disease burden and treatment response in malignant glioma. *Neuro Oncol.* **20**(4), 457–471. <https://doi.org/10.1093/neuonc/nox193> (2018).
- Lemee, J. M., Clavreul, A. & Menei, P. Intratumoral heterogeneity in glioblastoma: don't forget the peritumoral brain zone. *Neuro Oncol.* **17**(10), 1322–1332. <https://doi.org/10.1093/neuonc/nov119> (2015).
- Yan, J. et al. Multimodal MRI characteristics of the glioblastoma infiltration beyond contrast enhancement. *Ther Adv Neurol Disord.* <https://doi.org/10.1177/1756286419844664> (2019).
- Yamamoto, S. et al. Qualitative MR features to identify non-enhancing tumors within glioblastoma's T2-FLAIR hyperintense lesions. *J Neurooncol.* **165**(2), 251–259. <https://doi.org/10.1007/s11060-023-04454-9> (2023).
- Yamahara, T. et al. Morphological and flow cytometric analysis of cell infiltration in glioblastoma: A comparison of autopsy brain and neuroimaging. *Brain Tumor Pathol.* **27**(2), 81–87. <https://doi.org/10.1007/s10014-010-0275-7> (2010).
- Chenxing, Wu. et al. Peritumoral edema on magnetic resonance imaging predicts a poor clinical outcome in malignant glioma. *Oncol Lett.* **10**(5), 2769–2776. <https://doi.org/10.3892/ol.2015.3639> (2015).
- Wu, C. et al. Peritumoral edema shown by MRI predicts poor clinical outcome in glioblastoma. *World J Surg Oncol.* **11**(13), 97. <https://doi.org/10.1186/s12957-015-0496-7> (2015).
- Kauppinen, R. A. & Peet, A. C. Using magnetic resonance imaging and spectroscopy in cancer diagnostics and monitoring: Preclinical and clinical approaches. *Cancer Biol Ther.* **12**(8), 665–679. <https://doi.org/10.4161/cbt.12.8.18137> (2011).
- Siyah Mansoor, M. et al. Analysis of glioblastoma Multiforme tumor metabolites using Multivoxel magnetic resonance spectroscopy. *Avicenna J Med Biotechnol.* **12**(2), 107–115 (2020).
- Chaumeil, M. M., Lupo, J. M. & Ronen, S. M. Magnetic resonance (MR) metabolic imaging in glioma. *Brain Pathol.* **25**(6), 769–780. <https://doi.org/10.1111/bpa.12310> (2015).
- Czernicki, T. et al. Spectral changes in postoperative MRS in high-grade gliomas and their effect on patient prognosis. *Folia Neuropathol.* **47**(1), 43–49 (2009).
- Price, S. J. et al. Multimodal MRI can identify perfusion and metabolic changes in the invasive margin of glioblastomas. *J Magn Reson Imaging.* **43**(2), 487–494. <https://doi.org/10.1002/jmri.24996> (2016).
- Goryawala, M. et al. The association between whole-brain MR spectroscopy and IDH mutation status in gliomas. *J Neuroimaging.* **30**(1), 58–64. <https://doi.org/10.1111/jon.12685> (2020).
- Kazda, T. et al. Advanced MRI increases the diagnostic accuracy of recurrent glioblastoma: Single institution thresholds and validation of MR spectroscopy and diffusion weighted MR imaging. *Neuroimage Clin.* **26**(11), 316–321. <https://doi.org/10.1016/j.nicl.2016.02.016> (2016).
- Tolia, M. et al. Prognostic value of MRS metabolites in postoperative irradiated high grade gliomas. *Biomed Res Int.* **2015**, 341042. <https://doi.org/10.1155/2015/341042> (2015).
- Cepeda, S. et al. Predicting regions of local recurrence in glioblastomas using voxel-based radiomic features of multiparametric postoperative MRI. *Cancers (Basel)* **15**(6), 1894. <https://doi.org/10.3390/cancers15061894> (2023).

36. Cui, Y. et al. Higher Cho/NAA ratio in postoperative peritumoral Edema zone is associated with earlier recurrence of glioblastoma. *Front. Neurol.* **4**(11), 592155. <https://doi.org/10.3389/fneur.2020.592155> (2020).
37. Feng, A. et al. Distinguishing tumor recurrence from radiation necrosis in treated glioblastoma using multiparametric MRI. *Acad. Radiol.* **29**(9), 1320–1331. <https://doi.org/10.1016/j.acra.2021.11.008> (2022).

Acknowledgments

We would like to thank the Imaging Department of Ningxia Medical University for providing technical support

Author contributions

WL: Data analysis and draft the manuscript; JF: Data collection and validation; YL, XW and YZ: Data collection; PG and YRZ: Revise the manuscript; HM: Study design and supervision. All authors reviewed the manuscript.

Funding

This work was supported by the Ningxia NaturalScience Foundation of China (NO. 2022AAC03559).

Declarations

Competing interests

The authors declare no competing interests.

Additional information

Correspondence and requests for materials should be addressed to H.M.

Reprints and permissions information is available at www.nature.com/reprints.

Publisher's note Springer Nature remains neutral with regard to jurisdictional claims in published maps and institutional affiliations.

Open Access This article is licensed under a Creative Commons Attribution-NonCommercial-NoDerivatives 4.0 International License, which permits any non-commercial use, sharing, distribution and reproduction in any medium or format, as long as you give appropriate credit to the original author(s) and the source, provide a link to the Creative Commons licence, and indicate if you modified the licensed material. You do not have permission under this licence to share adapted material derived from this article or parts of it. The images or other third party material in this article are included in the article's Creative Commons licence, unless indicated otherwise in a credit line to the material. If material is not included in the article's Creative Commons licence and your intended use is not permitted by statutory regulation or exceeds the permitted use, you will need to obtain permission directly from the copyright holder. To view a copy of this licence, visit <http://creativecommons.org/licenses/by-nc-nd/4.0/>.

© The Author(s) 2024